Mesenchymal stem cells alleviated sepsis-induced acute lung injury by blocking NETs formation and inhibiting ferroptosis

TieNan Wang [Equal first author, 1], **Zheng Zhang** [Equal first author, 1], **ZhiZhao Deng** [1], **WeiQi Zeng** [1], **YingXin Gao** [1], **ZiQing Hei** [Corresp., 1], **DongDong Yuan** [Corresp. 1]

[1] Department of Anesthesiology, The Third Affiliated Hospitol of Sun Yat-Sen University, GuangZhou, GuangDong Province, China

Corresponding Authors: ZiQing Hei, DongDong Yuan
Email address: heiziqing@sina.com, yuandongdong123@126.com

Acute lung injury (ALI) is one of the most serious complications of sepsis with high morbidity and mortality. Ferroptosis has been reported playing an essential role in sepsis-induced ALI recently, however, the underlying mechanism was still unclear until now. Excessive neutrophil extracellular traps (NETs) formation would induce exacerbate inflammation and is vital to ALI. Thus, in present study, we explore the effects of ferroptosis or NETs on sepsis-induced ALI and observe the therapeutic function of mesenchymal stem cells (MSCs). We produced cecal ligation and puncture (CLP) model of sepsis in rats. Firstly, ferrostain-1 and DNase-1 were used to inhibit ferroptosis and NETs formation separately, to confirm their effects on sepsis-induced ALI. Secondly, U0126 was applicated to suppress MEK/ERK signaling pathway, considered to be vital of NETs formation. Finally, the therapeutic effect of MSCs was observed on CLP models. The results demonstrated that both ferrostain-1 and DNase-1 application could improve sepsis-induced ALI, and even more, DNase-1 also inhibited ferroptosis significantly in lung tissues, which showed that ferroptosis could be regulated by NETs formation. With the inhibition of MEK/ERK signaling pathway by U0126, NETs formation and ferroptosis in lung tissues were both attenuated, and sepsis-induced ALI was improved. MSCs also had a similar protective effect against on sepsis-induced ALI, not only inhibited MEK/ERK signaling pathway-mediated NETs formation, but also alleviated ferroptosis in lung tissues. We concluded that MSCs could protect against sepsis-induced ALI through suppressing NETs formation and ferroptosis in lung tissues. In this study, we not only found that NETs formation and ferroptosis were both potential therapeutic targets to improve sepsis-induced ALI, and also provided new evidence for the clinical application of MSCs in the treatment of sepsis-induced ALI.

Mesenchymal stem cells alleviated sepsis-induced acute lung injury by blocking NETs formation and inhibiting ferroptosis

Tienan Wang[1], Zheng zhang[1], Zhizhao Deng[2], Weiqi Zeng[3], Yingxin Gao[4], Ziqing Hei*, Dongdong Yuan*.

[1-4,] *Department of Anesthesiology, The Third Affiliated Hospital of Sun Yat-sen University, Guangzhou 510630, China.

Corresponding Author:
Dongdong Yuan
TianHe Road 600th The Third Affiliated Hospital of Sun Yat-sen University, Guangzhou 510630, China. E-mail address: yuandongdong123@126.com
Ziqing Hei,
TianHe Road 600th The Third Affiliated Hospital of Sun Yat-sen University, Guangzhou 510630, China. E-mail address: heiziqing@sina.com.

Abstract

Acute lung injury (ALI) is one of the most serious complications of sepsis with high morbidity and mortality. Ferroptosis has been reported playing an essential role in sepsis-induced ALI recently, however, the underlying mechanism was still unclear until now. Excessive neutrophil extracellular traps (NETs) formation would induce exacerbate inflammation and is vital to ALI. Thus, in present study, we explore the effects of ferroptosis or NETs on sepsis-induced ALI and observe the therapeutic function of mesenchymal stem cells (MSCs). We produced cecal ligation and puncture (CLP) model of sepsis in rats. Firstly, ferrostain-1 and DNase-1 were used to inhibit ferroptosis and NETs formation separately, to confirm their effects on sepsis-induced ALI. Secondly, U0126 was applicated to suppress MEK/ERK signaling

pathway, considered to be vital of NETs formation. Finally, the therapeutic effect of MSCs was observed on CLP models. The results demonstrated that both ferrostain-1 and DNase-1 application could improve sepsis-induced ALI, and even more, DNase-1 also inhibited ferroptosis significantly in lung tissues, which showed that ferroptosis could be regulated by NETs formation. With the inhibition of MEK/ERK signaling pathway by U0126, NETs formation and ferroptosis in lung tissues were both attenuated, and sepsis-induced ALI was improved. MSCs also had a similar protective effect against on sepsis-induced ALI, not only inhibited MEK/ERK signaling pathway-mediated NETs formation, but also alleviated ferroptosis in lung tissues. We concluded that MSCs could protect against sepsis-induced ALI through suppressing NETs formation and ferroptosis in lung tissues. In this study, we not only found that NETs formation and ferroptosis were both potential therapeutic targets to improve sepsis-induced ALI, and also provided new evidence for the clinical application of MSCs in the treatment of sepsis-induced ALI.

Key words:

sepsis, acute lung injury, mesenchymal stem cells, ferroptosis, neutrophil extracellular traps .

Introduction

Although additional progress has been made, sepsis is still a life-threatening multi-organ dysfunction caused by a body disordered response to infection (Reinhart et al. 2017). Secondarily acute lung injury (ALI) is a common clinical feature in patients with sepsis, which is also strongly associated with high morbidity and mortality (Prescott & Angus 2018). Acute respiratory distress syndrome (ARDS) causes inflammation of the alveolar-capillary membrane and pulmonary edema, is the most severe form of ALI. However, it is regrettable that up to now, the relevant mechanism of ALI caused by sepsis is still unclear, which leads to the lack of clinical treatment methods for it. Therefore, it is urgent to clarify the relevant mechanism of sepsis-induced ALI and look for potential therapeutic methods based on it.

Polymorphonuclear neutrophils (PMNs) are the dominating inflammatory cells recruited to lungs in sepsis, playing a central role in the pathogenesis of sepsis-induced ALI (Grommes & Soehnlein 2011). PMNs assail microorganisms after migrating to the infectious site by their ways: degranulation, phagocytosis or the release of NETs, the latter is webs of DNA material and antimicrobial proteins. At first, it's reported that the inhibition of NETs attenuated ALI

caused by intestinal ischemia reperfusion injury (Zhan et al. 2022). Recently, Alsabani M has proved that NETs formation lead to lung injury in human and murine sepsis and presented that reduction of NETs is a possible therapeutic target for endotoxic shock induced ALI (Alsabani et al. 2022). Nevertheless, little evidence is available on how NETs cause ALI/ARDS in sepsis. A study had confirmed that NETs-mediated ferroptosis of alveolar epithelial cells plays an important role in sepsis-induced ALI (Zhang et al. 2022). Known as a kind of cell death caused by lipid peroxidation and iron metabolism disorder, ferroptosis has been reported playing an essential role in sepsis-induced ALI recently (Shimizu et al. 2022), which might be potential target for lung tissue protection in sepsis .

There are few pharmacologic therapies proved both effective and low toxicity to improve sepsis-induced ALI so far. An exciting strategy to address this pressing need is the use of cell-based therapies, including MSCs. The potential for MSCs to alleviate and tissue repair in sepsis-induced ALI has been reported (Rojas et al. 2005). Although some understanding of the therapeutic mechanisms have been obtained, many are still unclear and some controversy persists, such as the effects of MSCs on NETs, ferroptosis, ALI or ARDS in sepsis. This results in the limit of MSCs clinical application. Therefore, in our present study, we focused on two major problems: the possible mechanisms of sepsis-induced ALI mediated by NETs or ferroptosis, and the protective effects of MSCs in this process.

In summary, we hypothesized that MSCs alleviated sepsis-induced ALI by inhibiting NETs-mediated ferroptosis. The relation between MSCs, NETs and ferroptosis was studied.

Materials & Methods

2.1 Animals

Healthy SPF (Sprague-Dawley, SD) male rats (200-250 g) were purchased from Hunan Skarjingda Co., LTD. Rats were raised in room temperature of 25 to 27°C and provided with a basic diet for one week prior to the experiments. All animal care and experimental protocols in this study were approved by the Institutional Animal Care and Use Committee of the Laboratory Animal Center of South China Agricultural University (Guangzhou, China) and were provided for laboratory animal use in accordance with National Institutes of Health Guidelines (NIH Publication 86-23 revised 1985).

2.2 Experimental Design

A total of 60 rats were housed in filtered-air ventilated cages with a free access to food and drink in an environment with a 12-h light/dark cycle, temperature of 20-26 ° C. These SD rats were from Hunan SJA Laboratory Animal Co.，Ltd. In the first experiment, rats were randomized to sham group (n = 6) or CLP group (n = 6), and lung tissue samples were collected at 24 h after surgery. The rats undergoing sham operation were subjected to ventral midline incision, sterilized and sutured, and given the same amount of fluid in CLP group. In another experiment, the rats were randomly assigned into three groups (n = 6 in each group), and the effects of ferrostatin-1, DNAse-1, and U0126 (specific inhibitor of MEK1) were observed as follows: sham group, CLP group, and CLP + corresponding inhibitor treating group. Ferrostatin-1 (1 mg/kg, Med Chem Express, HY-100579, Shanghai, P. R. China)/DNAse-1 (5 mg/kg, Beijing Solarbio Science & Technology Co., Ltd, 9003-98-9, Beijing, China)/U0126 (100 μg/kg, ABSIN, ABS810003, Shanghai, China). All inhibitors are configured according to the instructions, and the carrier refers to the corresponding solvent. Inhibitors mentioned above was administered by tail vein injection immediately after CLP modeling while Sham group and CLP group were treated with solvent of inhibitors. In another experiment, the rats were randomly assigned into three groups (n = 6 in each group). The effects of MSCS were observed as follows: sham group, CLP + vector group, and CLP + MSCs group. MSC ($5*10^6$ in 1 ml saline, mubmx-01001, Cyagen, Guangzhou, China) was injected through tail vein 1 h after CLP modeling. All rats received topical incision infiltration with 0.5% ropivacaine (1.0 mL/kg, AstraZeneca, USA) before laparotomy, plus a single subcutaneous administration of ketoprofen (40 mg/kg, Sigma-Aldrich Corp., St. Louis, MO)after abdominal closure for postoperative analgesia. Rats underwent CLP operation featured malaise, chills, generalized weakness and reduced gross motor and usually dead when inability to stand and breathe. When rats about to die were found or 24h after CLP modeling, rats were anesthetized with 3-5% isoflurane and euthanized by exsanguination. Samples were then collected. Only rats survived to 24h after modeling were included in the statistical analysis.

2.3 Rat cecal ligation and puncture model

All procedures involving animals in the rat caecal ligation and puncture model were performed in accordance with the guidelines for Animal experiments and were approved by the

Institutional Animal Care and Use Committee of South China Agricultural University (Approval No. 2022D010). According to the results of the preliminary experiment, the cecal ligation and puncture of rats were modified to ligation 75% and punctured 2 holes.

2.4 Treatment of mesenchymal stem cells

Adult bone marrow mesenchymal stem cells purchased from Saiye were cultured in OriCell® adult bone marrow mesenchymal stem cells complete medium (Cyagen, HuxMA-90011, Guangzhou, China). The seventh passage was digested, collected, counted and centrifuged. An appropriate amount of William's solution was added and resuspended to a concentration of 5*106/ml. Used in animal experiments.

2.5 Inhibitor treatment

The ferroptosis inhibitor group was treated with ferrostatin-1 (1 mg/kg, Med Chem Express, HY-100579, Shanghai, China) immediately after the same CLP modeling. The NETs inhibitor group was treated with DNASE-1 (100 μg/kg, Beijing Solarbio Science & Technology Co., Ltd, 9003-98-9, Beijing, China) at 1 hour after modeling. The MEK/ERK pathway inhibition group was treated with U0126 (100 μg/kg, ABSIN, ABS810003, Shanghai, China) immediately after modeling.

2.6 Hematoxylin and eosin staining

As indicated in the experimental design, the rats were sacrificed 24h after CLP modeling and lung tissues were harvested. The left lung was used to determine the dry/wet ratio, and the right middle lobe was fixed with formaldehyde and embedded in paraffin for subsequent hematoxylin and eosin staining. The pathological changes of lung tissue were observed under light microscope. Two pathologists scored sepsis-induced ALI based on the assessment criteria described in our previous study.

2.7 Dry/wet ratio

The left lobe was used in the dry/wet ratio experiment. After dissection, the left hilus was ligated, and the whole left lobe was cut off and put into a clean and weighed centrifuge tube to measure the wet weight. Then the left lobe was placed in a Petri dish and placed in a 60℃ oven

to measure the dry weight after drying for 48 hours. The ratio of wet weight to dry weight was taken as the final result.

2.8 Immunohistochemistry

Paraffin embedded blocks of the right middle lobe were sliced into 5 μm thick and stained with rabbit anti-rat ACSL4 (1:100, ABclonal, A6826, China). The expression of ACSL4 in lung tissue was detected by HRP rabbit secondary antibody. The sections were deparaffinized with xylene, dehydrated with ethanol, and then heated in 0.01 M citrate buffer (pH 6.0). Endogenous peroxidase activity was inactivated in 3% H2O2 for 15 minutes at RT. After the sections were incubated in blocking buffer (10% goat serum albumin), they were incubated with primary antibodies recognizing ACSL4 (1:100, ABclonal, A6826, China) at 4℃ overnight. Then, the tissues were incubated with secondary anti-rabbit antibody-coated polymer peroxidase complexes (Beyotime, A0208, NanJing, China) at RT. After the tissues were incubated with chromogenic substrates DAB (Beyotime, P0203, Nan Jing, China) for 1 min, the slides were incubated with hematoxylin (Beyotime, C0107, Nan Jing, China) for 10 seconds. The sections were washed in running water for 20 minutes. Under optical microscope, five fields per each slide at random choice of the viewer were semi-quantified.

2.9 Immunofluorescence & Immunofluorescence radiography

The right upper lobe was embedded with OCT embedding agent and were cut into 5-lm sections; potential non-specific staining in the sections was blocked with 5% goat serum albumin and 0.1% Triton X-100 in PBS. Rabbit Histone H3Rb mAb (1:200, ABCAM, AB219407, USA) and Mouse MPO Mb mAb (1:100, Immunoway, YM33964, TX, USA) primary anti-bodies were used to binding antigen. Then Dylight488, Goat Anti Rabbit IgG /Dylight594 Goat Anti Mouse IgG secondary antibody (1:500, Immunoway, RS23220; RS3608, USA) were fluorescent-labeled to detect the expression of neutrophil extracellular traps. Laser confocal microscope (Zeiss, LSM880, German) was utilized for observing the stained sections. Z-stack model was used to catch several pictures from different depth at a same area. Maximum efficiency overlay was used to establish a final picture. Image J1.48(National Institutes of Health) was used to calculate the fluorescence intensity, area and neutrophil count after Photoshop and standard Image processing.

2.10 Immunoblotting.

Western blotting was performed following standard procedures. Anti-ACSL4 antibody (1:1000, A16848, ABclonal), anti-ferritin Heavy Chain (FTH) antibody (1:1000; 381204, Zen Bio), anti-GPX4 antibody (1:5000; ab125066, Abcam), anti- ERK1/2 antibody (1:2000; YT1625, Immunoway), anti- Phospho-Erk1/2 antibody (1:2000; O1923, Cell Signaling), anti-MEK1/2 antibody (1:2000; D1A5, Cell Signaling), anti-Phospho-MEK1/2 antibody (1:2000; 41G9, Cell Signaling) and secondary antibody (1:2000; Beyotime) were used to detect protein expression. Anti-GAPDH (Zen Bio) were used at 1:2000. Images were acquired by a Tanon 5500 imaging system (Tanon, Shanghai). The images were scanned with the Image J scanning software, and the data were expressed as relative values to sham or control values.

2.11 Determination of iron ion, GSH and MDA in tissues

About 1 mg of tissue blocks were taken under dry ice and mechanically homogenized using zirconia beads. Tissue iron concentration was detected according to the experimental protocol of Nanjing Jiancheng Kit. The concentrations of GSH and MDA in tissues were detected according to the Nanjing Biyuntian Kit test protocol.

2.12 ELISA

About 1mg tissue block was taken under dry ice environment and mechanical homogenization was performed with metal beads in PBS medium. The concentrations of TNF-α, IL-6, IL-10 and MPO (JINGMEI JINGMEI Biological, JM-01597R1) in lung tissue homogenate were detected. We used MPO to represent neutrophil Nets net levels in lung tissue.

2.13 Statistical Analysis

Each biological experiment was performed in at least three replicates. Results were expressed as mean ±SEM. Differences between two groups were analyzed by indepentent samples t test and between above two groups were analyzed by one-way analysis of variance. Turkey's test is used for further comparison. The histopathological score did not fit a normal distribution and was analyzed by non-parametric tests. GraphPad Prism 6 software was used for statistical analysis of all experimental data, and $p < 0.05$ was used as the threshold for statistical significant differences.

.

Results

3.1 Ferroptosis involved in sepsis-induced ALI

Pathological damage, pulmonary edema and inflammation occurred in sepsis-induced ALI, manifested as higher histopathological scores, W/D ratio, tissue TNF-α level and IL-6 level in CLP group (Fig. 1A-1D). The protein expression of achaete-scute family BHLH transcription factor 4 (ACSL4), glutathione peroxidase 4 (GPX4), ferritin heavy chain (FTH), and the level of glutathione (GSH), malondialdehyde (MDA) and Fe2+ in lung tissue are all important indicators reflecting the degree of ferroptosis (Dixon et al. 2012). We found that GSH and GPX4 expression decreased and FTH showed no significance change in CLP group while all the other ferroptosis related indicators mentioned above increased significantly in CLP group, indicating that ferroptosis became more severe in sepsis-induced ALI and might play an important part in ALI (Fig. 1E-1H). After the treatment of fer-1 in septic rats, an ferroptosis inhibitor, the expression of ACSL4, MDA and cell free Fe2+ in lung tissue decreased apparently, and the expression of GPX4, FTH and GSH was improved (Fig. 2A-2D), while pathological damage, pulmonary edema and inflammation were restored (Fig. 2E-2H). All these results suggested that inhibiting ferroptosis attenuated sepsis-induced ALI.

3.2 Inducing NETs depletion suppressed ferroptosis

In recent years, different reports demonstrated that NETs is a new mechanism of alveolar epithelial cell injury (Scozzi et al. 2022). Therefore, we explored the changes of NETs in lungs and its function on lung ferroptosis. Fig. 3A-3C showed that a large number of NETs emerged in lung tissue in CLP group. The representative indicators, such as MPO and Histone H3 were both increased. After the treatment of Dnase-1 to induce NETs depletion, ferroptosis in sepsis-induced ALI was suppressed: the expression of ACSL4 and the level of MDA and cell free Fe2+ in lung tissue decreased, and the downregulation of GPX4, FTH and GSH expression caused by CLP was reversed (Fig. 3D-3G). Thus, we concluded that NETs depletion could decreased lung ferroptosis.

3.3 Suppressing MEK/ERK pathway alleviated NETs formation and alleviated ferroptosis-induced ALI in sepsis

In Fig. 4, we detected the changes of MEK/ERK signaling pathway, considered to be the main cause of the NETs formation (Hakkim et al. 2011). The results showed that the phosphorylation levels of MEK and ERK significantly increased in CLP rats, which could be reversed by U0126, a MEK inhibitor (Fig. 4A-4B). More importantly, with the inhibition of MEK/ERK signaling pathway by U0126, the formation of NETs was significantly suppressed manifested as MPO and Histone depression (Fig. 4D-4E). Subsequently, we explored effects of U0126 on ferroptosis and lung injury. The results demonstrated that after inhibition of MEK/ERK signaling pathway by U0126 pretreatment, ferroptosis related indicators, such as ACSL4, MDA and cell free Fe2+ in lung tissue of CLP group, were all decreased, but GPX4, FTH and GSH expression was increased (Fig. 5E-5H). Histopathological scores, W/D ratio, tissue TNF-α and IL-6 levels were also alleviated (Fig. 5A-5D).

3.4 MSCs improved lung tissue ferroptosis and alleviated sepsis-induced ALI via blocking suppressing MEK/ERK pathway-induced NETs formation

Results above indicated that lung tissue ferroptosis mediated by MEK/ERK pathway-induced NETs may play an important part in sepsis-induced ALI. Therefore, in Fig. 6 and 7, we observed the role of MSCs on lung tissue ferroptosis and sepsis-induced ALI and determined whether its function was related with above mechanism. The results in Fig. 6 showed that after injection of MSCs, the phosphorylation level of MEK and ERK (p-MEK and p-ERK) significantly decreased in CLP rats (Fig. 6A-6B) and their downstream NETs formation was also partly blocked (Fig. 6C-6E). Additionally, because of MSCs injection, ferroptosis related indicators, such as ACSL4, MDA and cell free Fe2+ in lung tissue of CLP group, were all decreased, but GPX4, FTH, GSH expression was increased (Fig. 7A-7D). With the depletion of NETs in lung tissue and the improvement of lung tissue ferroptosis, CLP-induced ALI was restored: histopathological scores, W/D ratio, tissue TNF-α and IL-6 levels were all alleviated (Fig. 7E-7H).

Discussion

There are some major findings in the present study. With the application of fer-1, Dnase-1 and U0126 to inhibit ferroptosis, NETs and MEK/ERK pathway respectively, we confirmed that MEK/ERK pathway could induce NETs formation and subsequently result in lung tissue

ferroptosis and even ALI. Meanwhile, we also provided a potential strategy to protect against sepsis-induced ALI, MSCs injection, which not only inhibited MEK/ERK pathway and its downstream NETs formation, but also attenuated lung tissue ferroptosis and sepsis-induced ALI (Fig. 8). This new findings have never been reported.

As a new form of regulated cell death triggered by erastin or RSL3, ferroptosis was first reported by Dixon in 2012(Dixon et al. 2012). Ferroptosis has been proved critical in sepsis-induced multiple organ injuries, including heart, liver and intestine. Different reports clarified thses kinds of organ injuries can be alleviated by the inhibition of ferroptosis (Li et al. 2021; Li et al. 2020a; Wang et al. 2020; Wei et al. 2020). Therefore, multiple researchers considered that ferroptosis inhibition might be a potential strategy in organ protection. However, the role of ferroptosis in sepsis-induced ALI is contradictory. On one hand, there were studies showing that the treatment of ferroptosis inducer could exacerbate alveolar inflammation and pulmonary edema, accompanied by cytokines increased obviously, while these effects could be reversed by ferroptosis inhibitor (Dong et al. 2020; Li et al. 2020b; Liu et al. 2020). On the other hand, it's also reported that erastin treatment, with the increase of ferroptosis, attenuated the inflammatory response and sepsis development (Oh et al. 2019). These results suggested that the function of ferroptosis in sepsis-induced ALI was still unclear. In our present study, we found that ferroptosis inhibitor treatment protected lung from sepsis-induced ALI, confirming that ferroptosis mainly had negative effect in sepsis-induced ALI.

As we know, PMNs play both vital and well-established role in sepsis-induced ALI. Besides regulating ALI through the production of reactive oxygen species (ROS) or executing degranulation and phagocytosis, PMNs have been highlighted in ALI pathogenesis by another way, which is named NETosis. NETs consist of a mix of neutrophil granule proteins, nuclear chromatin and mitochondrial DNA that primarily absolve a defensive role against infection (Lood et al. 2016; McIlroy et al. 2014; Neubert et al. 2018; Urban et al. 2009; Yousefi et al. 2009). Exuberant NETosis would promote microvascular dysfunction or even direct cellular/tissue injury (Silva et al. 2021). As a consequence, high levels of NETs in bronchoalveolar or peripheral blood are generally associated with the worst ARDS outcomes (Mikacenic et al. 2018; Pan et al. 2017). Although both NETs and ferroptosis have been proved

play an important part in sepsis-induced ALI, the relationship between them are still ambiguous. As we mentioned above, NETs have recently been reported regulating sepsis-associated ALI by activating ferroptosis in alveolar epithelial cells (Zhang et al. 2022). Our study confirmed that NETs developed excessively by the MEK/ERK pathway activation in the pathogenesis of sepsis-induced ALI, and the impairment of NETs was partly relative with ferroptosis.

MSCs can be isolated from many types of mesenchymal tissue, such as bone marrow, umbilical cord blood, adipose tissue, placenta and so on (Chamberlain et al. 2007). MSCs had been reported to mediate potent immunomodulation to influence both innate and adaptive immune cells, and this represented an important mechanism underlying the benefits of cell-based treatment for sepsis-induced ALI, rather than the paradigm of trans-differentiation as well as cell replacement. Although the possible benefits of MSCs for treating sepsis-induced ALI had already been investigated, the concrete mechanisms remained vague (Lee et al. 2011), which severely limits its clinical application to treat sepsis-induced ALI. Increasing studies including our present one had clarified that both NETs and ferroptosis were critical in the pathogenesis of sepsis-induced ALI (Qu et al. 2022; Qu et al. 2021; Scozzi et al. 2022; Zhang et al. 2021). However, the relation between MSCs, NETs and ferroptosis remained unclear. In our present study, we proved that MSCs injection alleviated sepsis-induced ALI significantly, and its underlying mechanism might be relative with MSCs blocking the formation of NETs and its downstream ferroptosis through inactivating MEK/ERK pathway. We believe that our research not only clarifies the mechanism of sepsis-induced ALI, but also provides a new theoretical basis for the clinical application of MSCs.

Conclusions

Our findings showed that the treatment of MSCs could effectively alleviate sepsis-induced ALI, and the probably underlying mechanisms were blocking the NETs formation as well as inhibiting ferroptosis.

Acknowledgements

This research was supported by the National Natural Science Foundation of China (NO. 82072216, 81871597); Natural Science Foundation of Guangzhou City (NO. 202102020167),

Basic and Applied Basic Research Foundation of Guangdong Province (NO. 2019A1515010093, 2021A1515111153, 2022A1515012611, 2022A1515011556)

References

Alsabani MA, S. T.&Cheng, Z. (2022).Alsabani M, Abrams ST, Cheng Z, Morton B, Lane S, Alosaimi S, Yu W, Wang G, and Toh CH Reduction of NETosis by targeting CXCR1/2 reduces thrombosis, lung injury, and mortality in experimental human and murine sepsis. *Br J Anaesth* 128:283-293. 10.1016/j.bja.2021.10.039

Chamberlain G (2007).Chamberlain G, Fox J, Ashton B, and Middleton J Concise review: mesenchymal stem cells: their phenotype, differentiation capacity, immunological features, and potential for homing. *Stem Cells* 25:2739-2749. 10.1634/stemcells.2007-0197

Dixon SJ (2012).Dixon SJ, Lemberg KM, Lamprecht MR, Skouta R, Zaitsev EM, Gleason CE, Patel DN, Bauer AJ, Cantley AM, Yang WS, Morrison B, 3rd, and Stockwell BR Ferroptosis: an iron-dependent form of nonapoptotic cell death. *Cell* 149:1060-1072. 10.1016/j.cell.2012.03.042

Dong HQ, Z. (2020).Dong H, Qiang Z, Chai D, Peng J, Xia Y, Hu R, and Jiang H Nrf2 inhibits ferroptosis and protects against acute lung injury due to intestinal ischemia reperfusion via regulating SLC7A11 and HO-1. *Aging (Albany NY)* 12:12943-12959. 10.18632/aging.103378

Grommes J (2011).Grommes J, and Soehnlein O Contribution of neutrophils to acute lung injury. *Mol Med* 17:293-307. 10.2119/molmed.2010.00138

Hakkim A (2011).Hakkim A, Fuchs TA, Martinez NE, Hess S, Prinz H, Zychlinsky A, and Waldmann H Activation of the Raf-MEK-ERK pathway is required for neutrophil extracellular trap formation. *Nat Chem Biol* 7:75-77. 10.1038/nchembio.496

Lee JW (2011).Lee JW, Fang X, Krasnodembskaya A, Howard JP, and Matthay MA Concise review: Mesenchymal stem cells for acute lung injury: role of paracrine soluble factors. *Stem Cells* 29:913-919. 10.1002/stem.643

Li JL, K. (2021).Li J, Lu K, Sun F, Tan S, Zhang X, Sheng W, Hao W, Liu M, Lv W, and Han W Panaxydol attenuates ferroptosis against LPS-induced acute lung injury in mice by Keap1-Nrf2/HO-1 pathway. *J Transl Med* 19:96. 10.1186/s12967-021-02745-1

Li NW, W. (2020a).Li N, Wang W, Zhou H, Wu Q, Duan M, Liu C, Wu H, Deng W, Shen D, and Tang Q Ferritinophagy-mediated ferroptosis is involved in sepsis-induced cardiac injury. *Free Radic Biol Med* 160:303-318. 10.1016/j.freeradbiomed.2020.08.009

Li YC, Y.&Xiao, J. (2020b).Li Y, Cao Y, Xiao J, Shang J, Tan Q, Ping F, Huang W, Wu F, Zhang H, and Zhang X Inhibitor of apoptosis-stimulating protein of p53 inhibits ferroptosis and alleviates intestinal ischemia/reperfusion-induced acute lung injury. *Cell Death Differ* 27:2635-2650. 10.1038/s41418-020-0528-x

Liu P (2020).Liu P, Feng Y, Li H, Chen X, Wang G, Xu S, Li Y, and Zhao L Ferrostatin-1 alleviates lipopolysaccharide-induced acute lung injury via inhibiting ferroptosis. *Cell Mol Biol Lett* 25:10. 10.1186/s11658-020-00205-0

Lood CB, L. P. (2016).Lood C, Blanco LP, Purmalek MM, Carmona-Rivera C, De Ravin SS, Smith CK, Malech HL, Ledbetter JA, Elkon KB, and Kaplan MJ Neutrophil extracellular traps enriched in oxidized mitochondrial DNA are interferogenic and contribute to lupus-like disease. *Nat Med* 22:146-153. 10.1038/nm.4027

McIlroy DJ (2014).McIlroy DJ, Jarnicki AG, Au GG, Lott N, Smith DW, Hansbro PM, and Balogh ZJ Mitochondrial DNA neutrophil extracellular traps are formed after trauma and subsequent surgery. *J Crit Care* 29:1133 e1131-1135. 10.1016/j.jcrc.2014.07.013

Mikacenic C (2018).Mikacenic C, Moore R, Dmyterko V, West TE, Altemeier WA, Liles WC, and Lood C Neutrophil extracellular traps (NETs) are increased in the alveolar spaces of patients with ventilator-associated pneumonia. *Crit Care* 22:358. 10.1186/s13054-018-2290-8

Neubert EM, D. (2018).Neubert E, Meyer D, Rocca F, Gunay G, Kwaczala-Tessmann A, Grandke J, Senger-Sander S, Geisler C, Egner A, Schon MP, Erpenbeck L, and Kruss S Chromatin swelling drives neutrophil extracellular trap release. *Nat Commun* 9:3767. 10.1038/s41467-018-06263-5

Oh BML, S. J. (2019).Oh BM, Lee SJ, Park GL, Hwang YS, Lim J, Park ES, Lee KH, Kim BY, Kwon YT, Cho HJ,

and Lee HG Erastin Inhibits Septic Shock and Inflammatory Gene Expression via Suppression of the NF-kappaB Pathway. *J Clin Med* 8. 10.3390/jcm8122210

Pan B (2017).Pan B, Alam HB, Chong W, Mobley J, Liu B, Deng Q, Liang Y, Wang Y, Chen E, Wang T, Tewari M, and Li Y CitH3: a reliable blood biomarker for diagnosis and treatment of endotoxic shock. *Sci Rep* 7:8972. 10.1038/s41598-017-09337-4

Prescott HC (2018).Prescott HC, and Angus DC Postsepsis Morbidity. *JAMA* 319:91. 10.1001/jama.2017.19809

Qu M (2022).Qu M, Chen Z, Qiu Z, Nan K, Wang Y, Shi Y, Shao Y, Zhong Z, Zhu S, Guo K, Chen W, Lu X, Wang Z, Zhang H, and Miao C Neutrophil extracellular traps-triggered impaired autophagic flux via METTL3 underlies sepsis-associated acute lung injury. *Cell Death Discov* 8:375. 10.1038/s41420-022-01166-3

Qu M (2021).Qu M, Zhang H, Chen Z, Sun X, Zhu S, Nan K, Chen W, and Miao C The Role of Ferroptosis in Acute Respiratory Distress Syndrome. *Front Med (Lausanne)* 8:651552. 10.3389/fmed.2021.651552

Reinhart K (2017).Reinhart K, Daniels R, Kissoon N, Machado FR, Schachter RD, and Finfer S Recognizing Sepsis as a Global Health Priority - A WHO Resolution. *N Engl J Med* 377:414-417. 10.1056/NEJMp1707170

Rojas M (2005).Rojas M, Xu J, Woods CR, Mora AL, Spears W, Roman J, and Brigham KL Bone marrow-derived mesenchymal stem cells in repair of the injured lung. *Am J Respir Cell Mol Biol* 33:145-152. 10.1165/rcmb.2004-0330OC

Scozzi D (2022).Scozzi D, Liao F, Krupnick AS, Kreisel D, and Gelman AE The role of neutrophil extracellular traps in acute lung injury. *Front Immunol* 13:953195. 10.3389/fimmu.2022.953195

Shimizu J (2022).Shimizu J, Murao A, Nofi C, Wang P, and Aziz M Extracellular CIRP Promotes GPX4-Mediated Ferroptosis in Sepsis. *Front Immunol* 13:903859. 10.3389/fimmu.2022.903859

Silva CMS (2021).Silva CMS, Wanderley CWS, Veras FP, Sonego F, Nascimento DC, Goncalves AV, Martins TV, Colon DF, Borges VF, Brauer VS, Damasceno LEA, Silva KP, Toller-Kawahisa JE, Batah SS, Souza ALJ, Monteiro VS, Oliveira AER, Donate PB, Zoppi D, Borges MC, Almeida F, Nakaya HI, Fabro AT, Cunha TM, Alves-Filho JC, Zamboni DS, and Cunha FQ Gasdermin D inhibition prevents multiple organ dysfunction during sepsis by blocking NET formation. *Blood* 138:2702-2713. 10.1182/blood.2021011525

Urban CF (2009).Urban CF, Ermert D, Schmid M, Abu-Abed U, Goosmann C, Nacken W, Brinkmann V, Jungblut PR, and Zychlinsky A Neutrophil extracellular traps contain calprotectin, a cytosolic protein complex involved in host defense against Candida albicans. *PLoS Pathog* 5:e1000639. 10.1371/journal.ppat.1000639

Wang C (2020).Wang C, Yuan W, Hu A, Lin J, Xia Z, Yang CF, Li Y, and Zhang Z Dexmedetomidine alleviated sepsis‐induced myocardial ferroptosis and septic heart injury. *Mol Med Rep* 22:175-184. 10.3892/mmr.2020.11114

Wei S (2020).Wei S, Bi J, Yang L, Zhang J, Wan Y, Chen X, Wang Y, Wu Z, Lv Y, and Wu R Serum irisin levels are decreased in patients with sepsis, and exogenous irisin suppresses ferroptosis in the liver of septic mice. *Clin Transl Med* 10:e173. 10.1002/ctm2.173

Yousefi S (2009).Yousefi S, Mihalache C, Kozlowski E, Schmid I, and Simon HU Viable neutrophils release mitochondrial DNA to form neutrophil extracellular traps. *Cell Death Differ* 16:1438-1444. 10.1038/cdd.2009.96

Zhan YL, Y.&Deng, Q. (2022).Zhan Y, Ling Y, Deng Q, Qiu Y, Shen J, Lai H, Chen Z, Huang C, Liang L, Li X, Wu J, Huang W, and Wen S HMGB1-Mediated Neutrophil Extracellular Trap Formation Exacerbates Intestinal Ischemia/Reperfusion-Induced Acute Lung Injury. *J Immunol* 208:968-978. 10.4049/jimmunol.2100593

Zhang HL, J.&Zhou, Y. (2022).Zhang H, Liu J, Zhou Y, Qu M, Wang Y, Guo K, Shen R, Sun Z, Cata JP, Yang S, Chen W, and Miao C Neutrophil extracellular traps mediate m(6)A modification and regulates sepsis-associated acute lung injury by activating ferroptosis in alveolar epithelial cells. *Int J Biol Sci* 18:3337-3357. 10.7150/ijbs.69141

Zhang HZ, Y.&Qu, M. (2021).Zhang H, Zhou Y, Qu M, Yu Y, Chen Z, Zhu S, Guo K, Chen W, and Miao C Tissue Factor-Enriched Neutrophil Extracellular Traps Promote Immunothrombosis and Disease Progression in Sepsis-Induced Lung Injury. *Front Cell Infect Microbiol* 11:677902. 10.3389/fcimb.2021.677902

Figure 1

Figure 1. Ferroptosis was involved in sepsis-induced ALI.

(A) HE staining of lung tissue from sham group and CLP group, scale bar = 50 μ m. (B) Pathological score of lung injury. According to neutrophil infiltration, alveolar tissue fragments, pathological cell proliferation, and degree of congestion, each item was scored as 3 points (>50%), 2 points (25-50%), 1 point (0-25%), and 0 point. (C) The dry to wet ratio of lung tissue was measured to compare lung-infiltrating humics (D) ELISA was performed for testing inflammatory factors. (E) Immunohistochemistry was performed to examine ACSL4 expression in rat lung tissue, scale bar = 50 μ m. (F) The relative IOD value of ACSL4. Each slice was compared with the average value of Sham group. (H) GSH, MDA and iron concentration. (G) The protein expression level of ferroptosis indicators ACSL4, GPX4, FTH in lung. Each bar represents the mean ± SEM (n = 6 per group). $^{*}p< 0.05$; $^{**}p < 0.01$; $^{***}p < 0.001$ one-way ANOVA with Tukey's test.

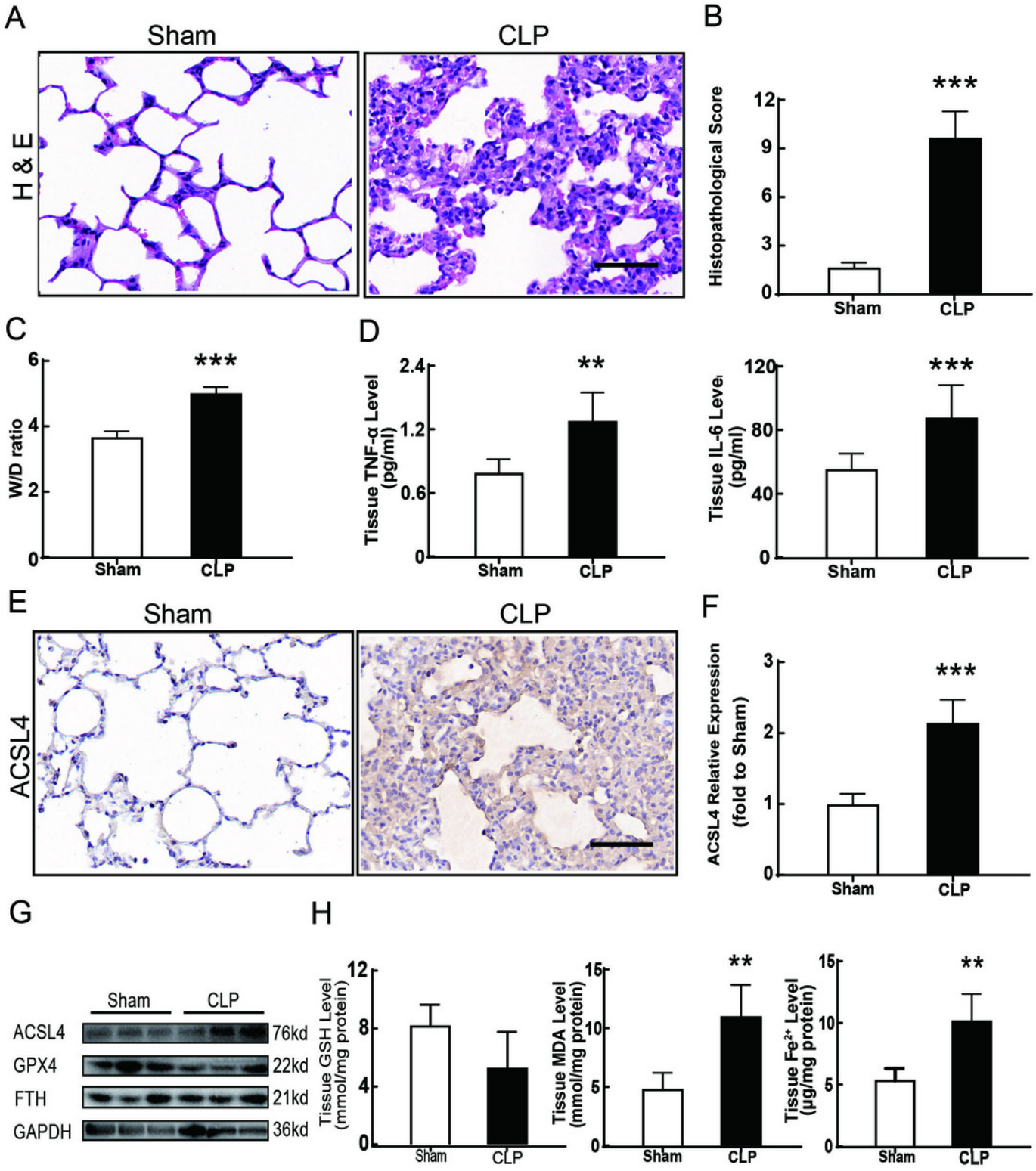
A
Sham
CLP
H & E
B
Histopathological Score
***
Sham
CLP
C
W/D ratio
***
Sham
CLP
D
Tissue TNF-α Level (pg/ml)
**
Sham
CLP
Tissue IL-6 Level (pg/ml)
***
Sham
CLP
E
Sham
CLP
ACSL4
F
ACSL4 Relative Expression (fold to Sham)
***
Sham
CLP
G
Sham
CLP
ACSL4
GPX4
FTH
GAPDH
76kd
22kd
21kd
36kd
H
Tissue GSH Level (mmol/mg protein)
Sham
CLP
Tissue MDA Level (mmol/mg protein)
**
Sham
CLP
Tissue Fe2+ Level (μg/mg protein)
**
Sham
CLP

Figure 2

Fig 2 Ferroptosis inhibitor Fer-1 alleviated ALI.

(A) ACSL4 Immunohistochemistry, scale bar = 50 μ m. (B)The relative IOD value of ACSL4. Each slice is compared with the average value of Sham group. (C) GSH, MDA and iron concentration in rat lung tissue. (D) The protein expression level of ACSL4, GPX4 and FTH level in lung. (E) HE staining for Sham group, CLP group and group with Fer-1 treatment after CLP modeling, scale bar = 50μ m. (F) Pathological score of lung injury. (G)The dry to wet ratio of lung tissue. (H) The level of inflammatory factors in lung tissue. Each bar represents the mean ± SEM (n = 6 per group). '*' means the group is compared with Sham group; '#' means the group is compared with CLP group, 'ns' means the group has no statistical differences to both Sham and CLP group.$^{*}p< 0.05$; $^{**}p < 0.01$; $^{***}p < 0.001$; $^{\#}p< 0.05$; $^{\#\#}p < 0.01$; $^{\#\#\#}p < 0.001$,one-way ANOVA with Tukey's test.

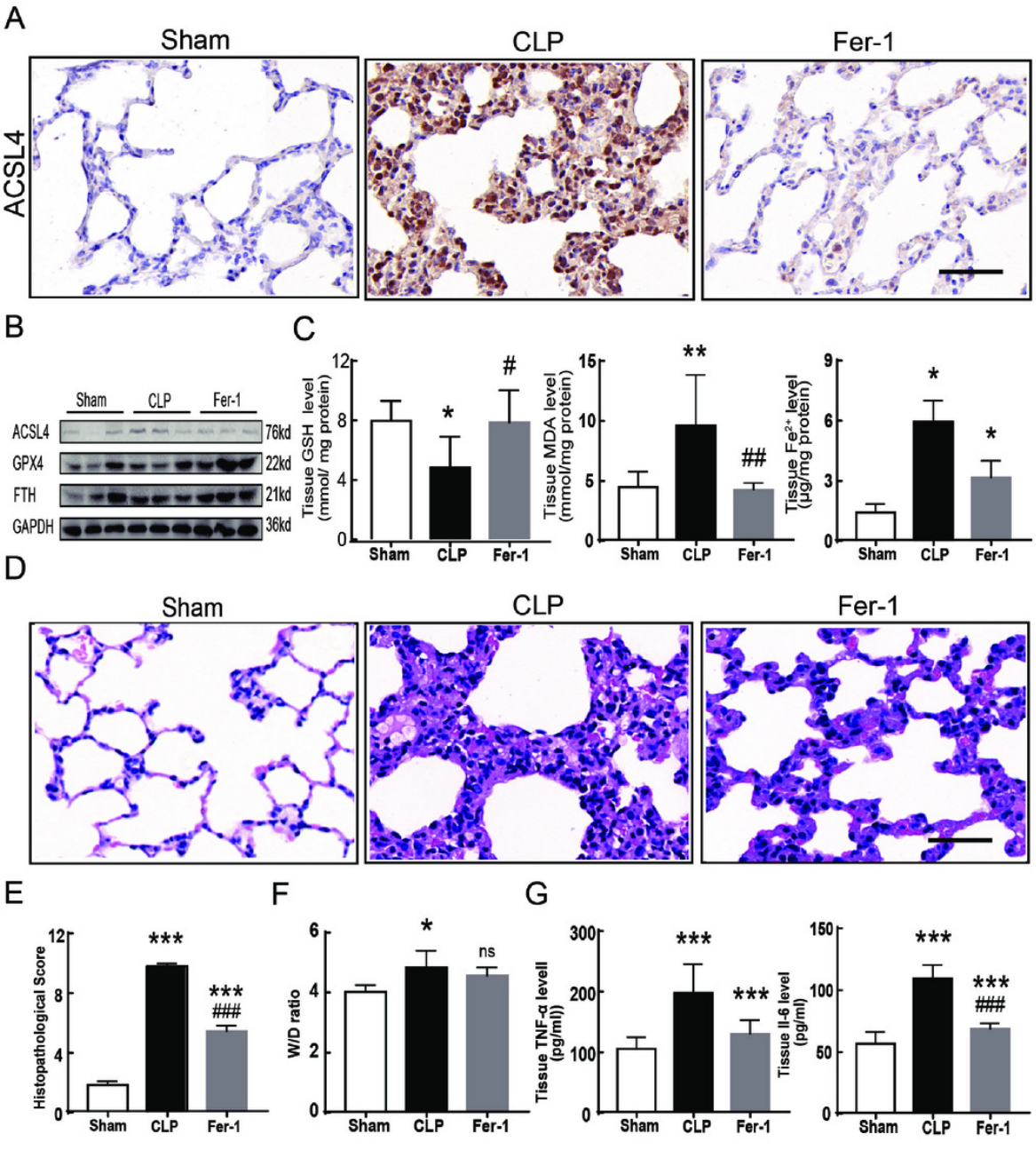
A
Sham
CLP
Fer-1
ACSL4
B
Sham
CLP
Fer-1
ACSL4
GPX4
FTH
GAPDH
76kd
22kd
21kd
36kd
C
Tissue GSH level (mmol/ mg protein)
Tissue MDA level (mmol/mg protein)
Tissue Fe2+ level (μg/mg protein)
D
E
Histopathological Score
F
W/D ratio
ns
G
Tissue TNF-α levell (pg/ml)
Tissue Il-6 level (pg/ml)

Figure 3

Fig 3 NETs inhibitor suppressed NETs formation and inhibited ferroptosis.

(A)Confocal microscope photography, scale bar=50 μ m. (B) The number of positive MPO markers represented neutrophil infiltration. The fomation of Nets was reperesented by The ratio of co-staining number to positive MPO numberrepresented NETosis. (C)ELISA represented semiquantitative NETs concentration in lung tissue. (D) ACSL4 Immunohistochemistry, scale bar = 50 μ m. (E) The relative IOD value of ACSL4. Each slice is compared with the average value of Sham group. (F) GSH, MDA and iron concentration in lung tissue. (G) The protein expression level of ACSL4, GPX4, FTH level in lung. Each bar represents the mean ± SEM (n = 6 per group). $^{*}p< 0.05$; $^{**}p < 0.01$; $^{***}p < 0.001$ one-way ANOVA with Tukey's test.

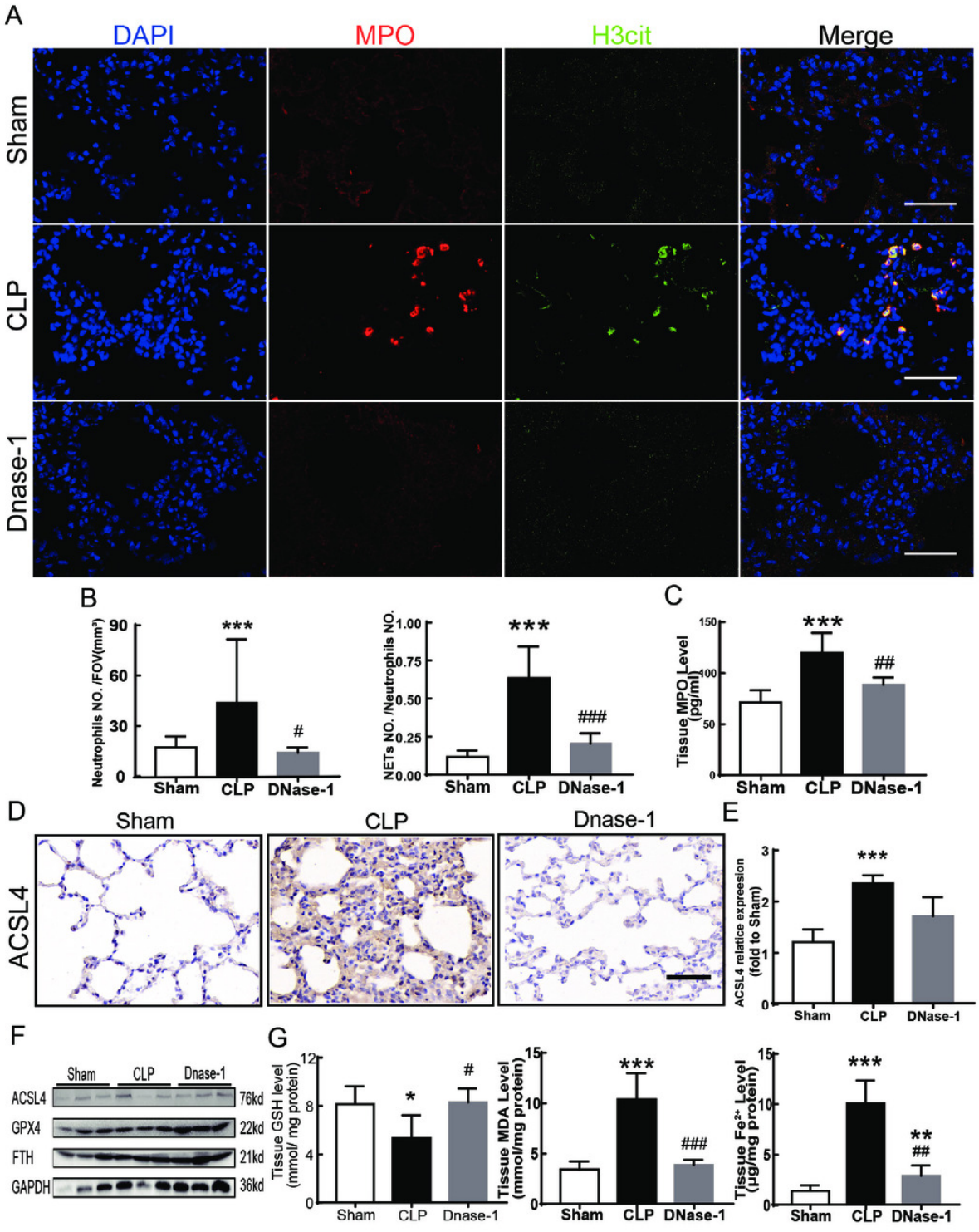
A
DAPI
MPO
H3cit
Merge
Sham
CLP
Dnase-1
B
Neutrophils NO. /FOV(mm²)
NETs NO. /Neutrophils NO.
Sham
CLP
DNase-1
C
Tissue MPO Level (pg/ml)
D
ACSL4
E
ACSL4 relatice expression (fold to Sham)
F
ACSL4
GPX4
FTH
GAPDH
76kd
22kd
21kd
36kd
G
Tissue GSH level (mmol/ mg protein)
Tissue MDA Level (mmol/mg protein)
Tissue Fe²⁺ Level (μg/mg protein)

Figure 4

Fig 4 MEK inhibitor U0126 inhibited MEK-ERK pathway activation and reduced NETosis.

(A) WB was used to detect The phosphorylation level of MEK and ERK. (B) IOD ratio of pMEK to MEK and pERK to ERK. (C) Immunofluorescence to examine NETosis, scale bar = 50 μ m. (D) Neutrophil inflitration and the degree of NETosis. (E) Semiquantitative NETs concentration in lung tissue. Each bar represents the mean ± SEM (n = 6 per group). $^{*}p< 0.05$; $^{**}p < 0.01$; $^{***}p < 0.001$ one-way ANOVA with Tukey's test.

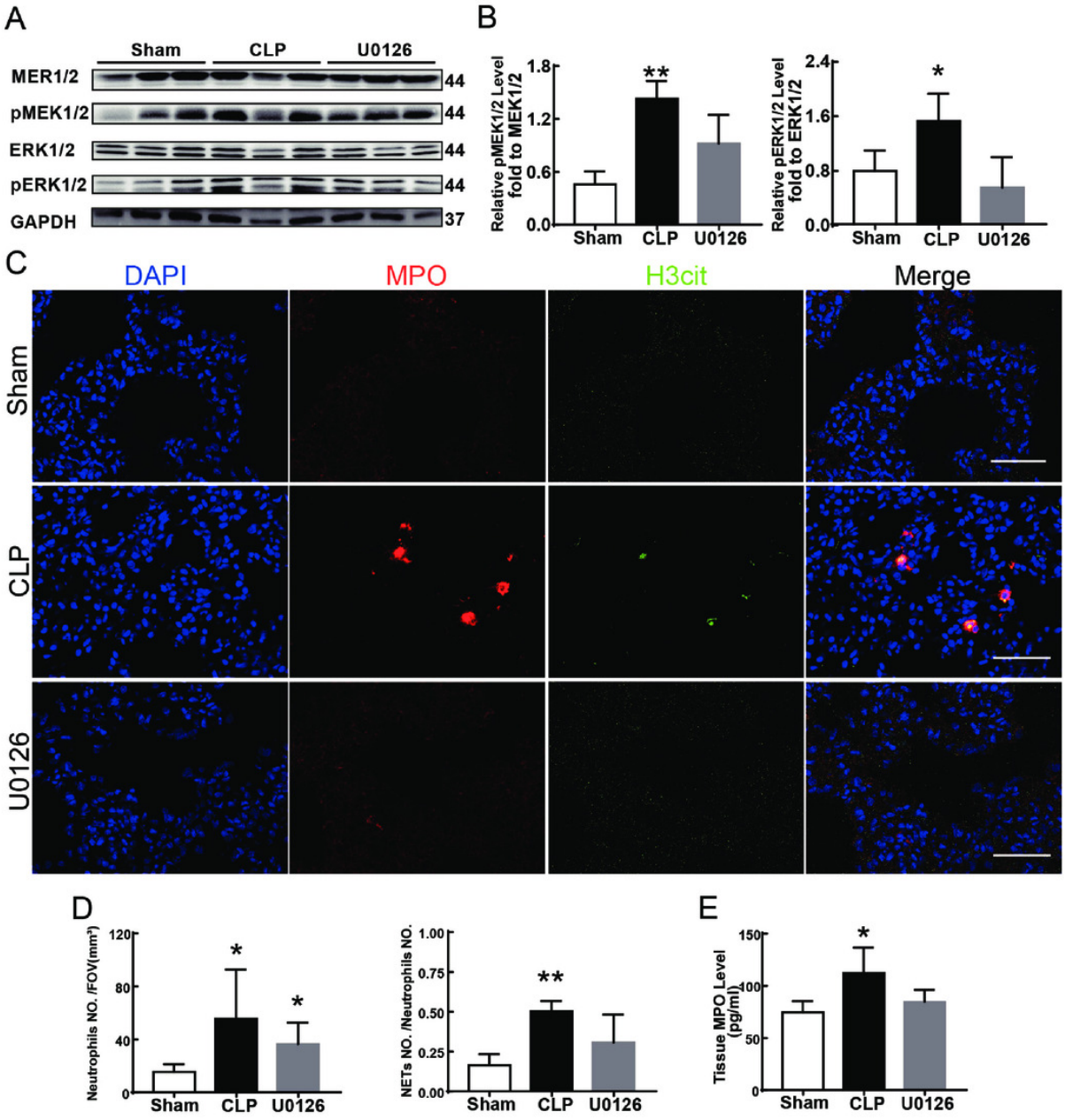
A
Sham
CLP
U0126
MER1/2
pMEK1/2
ERK1/2
pERK1/2
GAPDH
44
44
44
44
37
B
Relative pMEK1/2 Level fold to MEK1/2
Relative pERK1/2 Level fold to ERK1/2
Sham
CLP
U0126
C
DAPI
MPO
H3cit
Merge
Sham
CLP
U0126
D
Neutrophils NO. /FOV(mm²)
NETs NO. /Neutrophils NO.
E
Tissue MPO Level (pg/ml)

Figure 5

Figure 5. MEK inhibitor U0126 attenuated ALI and inhibited ferroptosis.

(A) HE staining for Sham group, CLP group and group with U0126 treatment after CLP modeling, scale bar = 50μ m. (B) Pathological score of lung injury. (C) The protein expression level of ACSL4, GPX4 and FTH in lung tissue. (D) The concentration of inflammatory factors in lungs. (E) ACSL4 Immunohistochemistry, scale bar = 50 μ m. (F) The relative IOD value of ACSL4. Each slice is compared with the average value of Sham group. (G)The dry to wet ratio of lung tissue. (H) The concentration of GSH, MDA and iron in lung tissue. Each bar represents the mean ± SEM (n = 6 per group). $^{*}p< 0.05$; $^{**}p < 0.01$; $^{***}p < 0.001$ one-way ANOVA with Tukey's test.

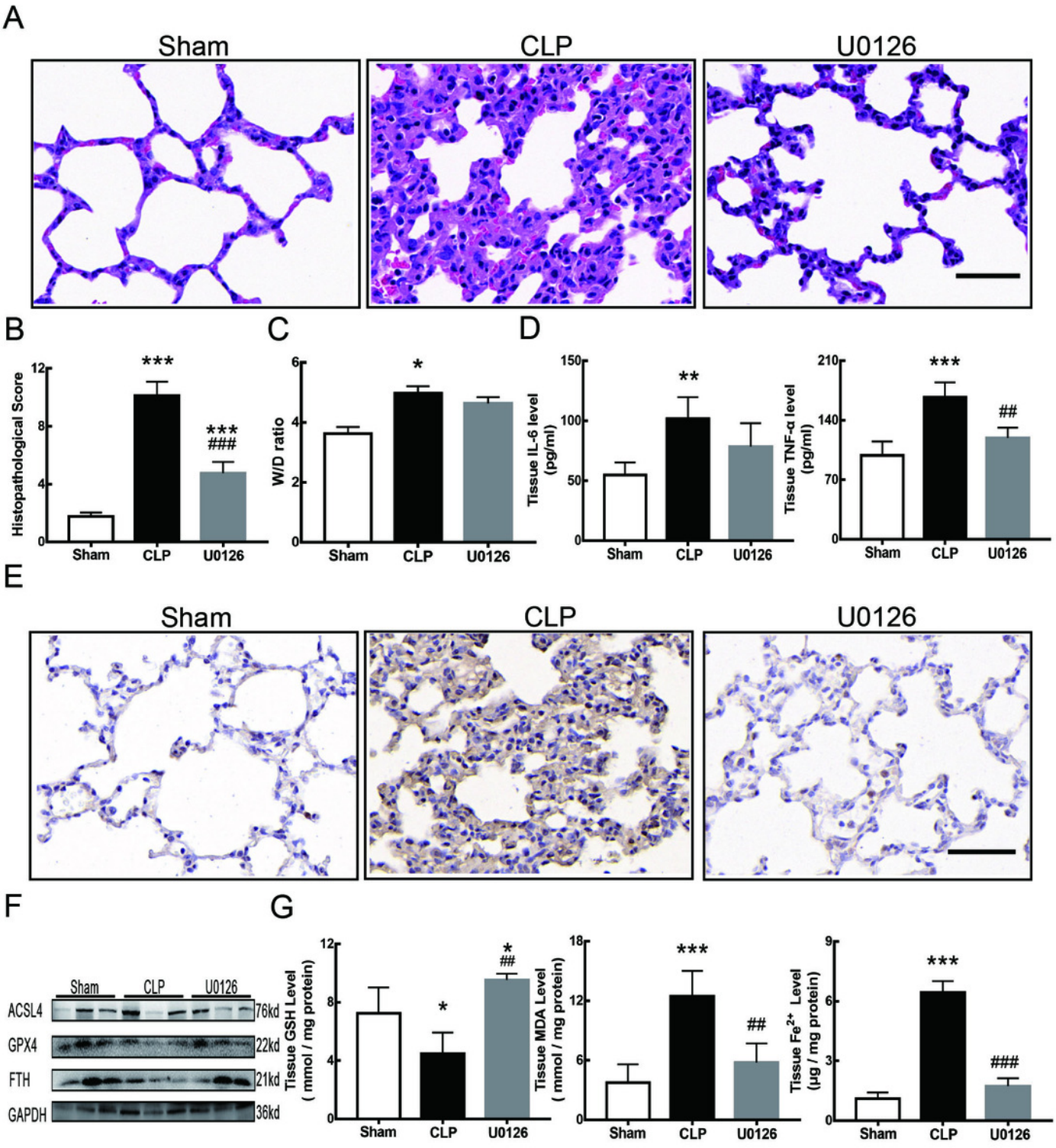
A
Sham
CLP
U0126
B
Histopathological Score
***
***
###
Sham
CLP
U0126
C
W/D ratio
*
Sham
CLP
U0126
D
Tissue IL-6 level (pg/ml)
**
Sham
CLP
U0126
Tissue TNF-α level (pg/ml)
***
##
Sham
CLP
U0126
E
Sham
CLP
U0126
F
Sham
CLP
U0126
ACSL4
76kd
GPX4
22kd
FTH
21kd
GAPDH
36kd
G
Tissue GSH Level (mmol / mg protein)
*
*
##
Sham
CLP
U0126
Tissue MDA Level (mmol / mg protein)
***
##
Sham
CLP
U0126
Tissue Fe2+ Level (μg / mg protein)
***
###
Sham
CLP
U0126

Figure 6

Fig 6 MSC inhibited MEK/ERK pathway activation and suprressed NETosis.

(A)The phosphorylation level of MEK and ERK. (B) IOD ratio of pMEK to MEK, and pERK to ERK. (C) Immunofluorescence for examining NETosis, scale bar=50 μ m. (D) Neutrophil inflitration and the degree of NETosis. (E) Semiquantitative Nets concentration in lung tissue. Each bar represents the mean ± SEM (n = 6 per group). $^{*}p< 0.05$; $^{**}p < 0.01$; $^{***}p < 0.001$ one-way ANOVA with Tukey's test.

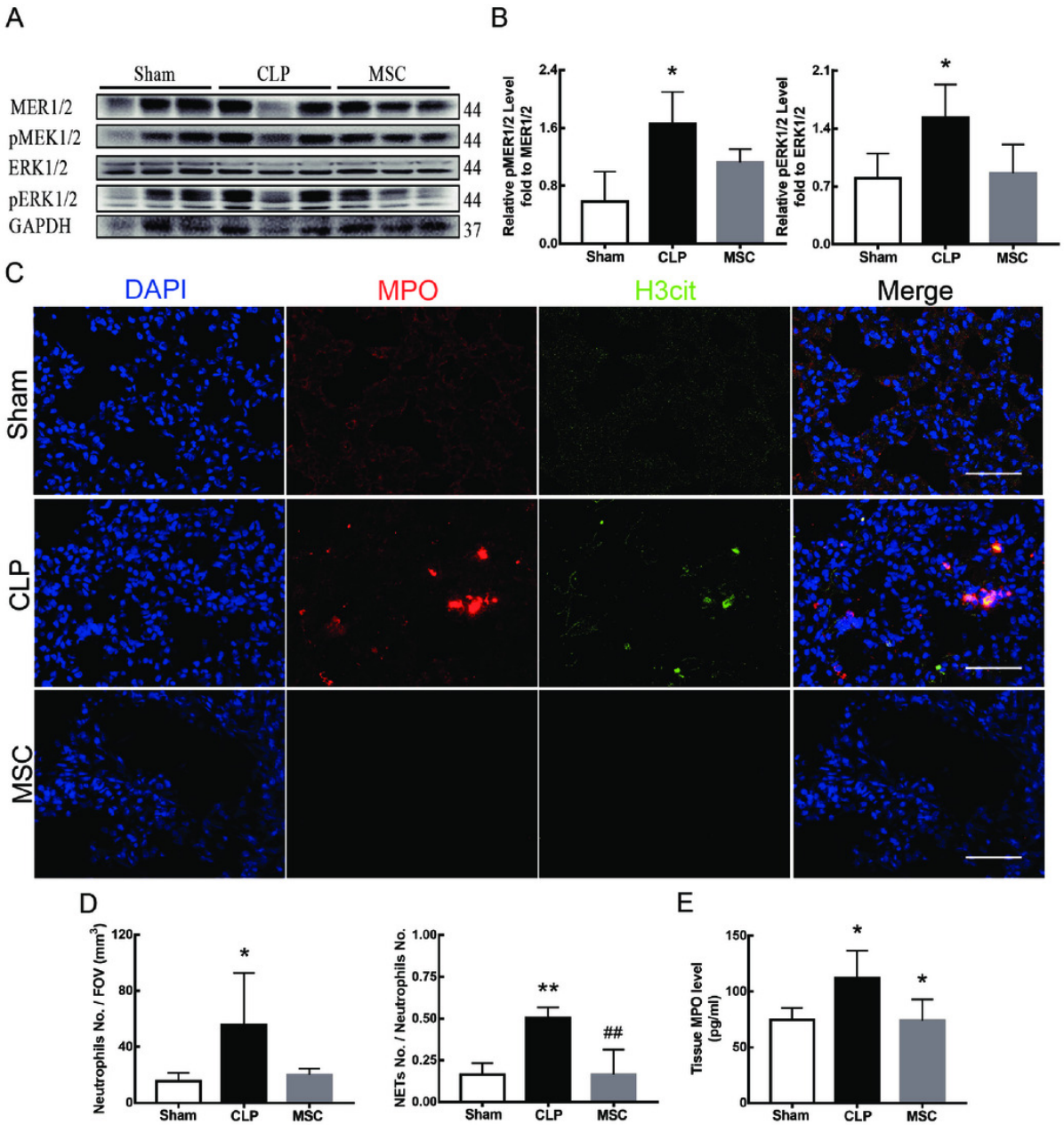
A
Sham
CLP
MSC
MER1/2
pMEK1/2
ERK1/2
pERK1/2
GAPDH
44
44
44
44
37
B
Relative pMER1/2 Level fold to MER1/2
Relative pERK1/2 Level fold to ERK1/2
Sham
CLP
MSC
C
DAPI
MPO
H3cit
Merge
Sham
CLP
MSC
D
Neutrophils No. / FOV (mm3)
NETs No. / Neutrophils No.
E
Tissue MPO level (pg/ml)

Figure 7

Figure 7. MSC inhibited ferroptosis and alleviated ALI.

(A) HE staining for Sham group, CLP group and group with MSC treatment after CLP modeling, scale bar = 50μ m. (B) Pathological score of lung injury. (C) The protein expression level of ACSL4, GPX4 and FTH level in lung tissue. (D) The concentration of inflammatory factors in lung tissue. (E) ACSL4 Immunohistochemistry, scale bar = 50 μ m. (F) The relative IOD value of ACSL4. Each slice is compared with the average value of Sham group. (G)The dry to wet ratio of lung tissue. (H) The concentration of GSH, MDA and iron in lung tissue.

Each bar represents the mean ± SEM (n = 6 per group). $^{*}p< 0.05$; $^{**}p < 0.01$; $^{***}p < 0.001$ one-way ANOVA with Tukey's test.

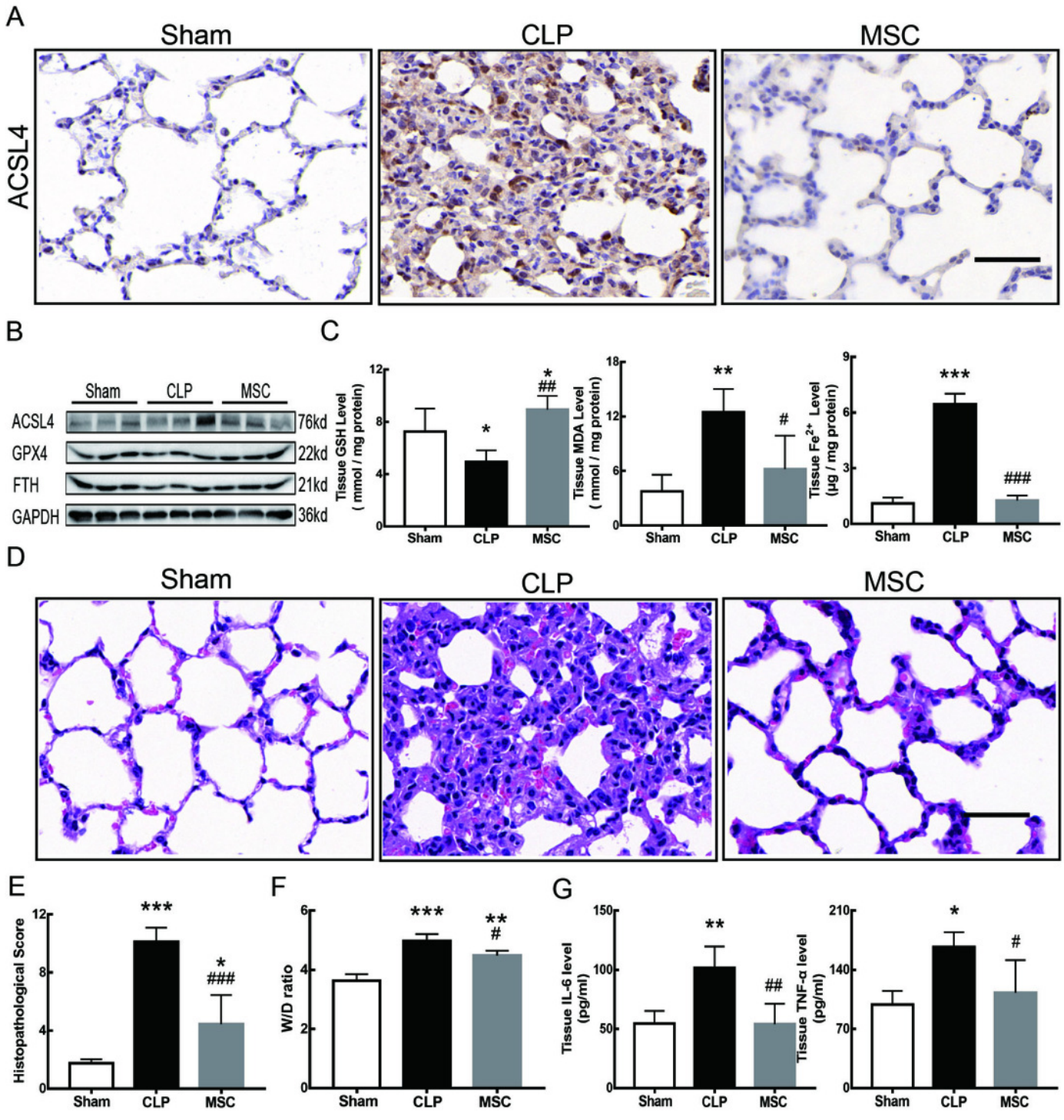
A
Sham
CLP
MSC
ACSL4
B
Sham
CLP
MSC
ACSL4
GPX4
FTH
GAPDH
76kd
22kd
21kd
36kd
C
Tissue GSH Level (mmol / mg protein)
Tissue MDA Level (mmol / mg protein)
Tissue Fe2+ Level (μg / mg protein)
D
Sham
CLP
MSC
E
Histopathological Score
F
W/D ratio
G
Tissue IL-6 level (pg/ml)
Tissue TNF-α level (pg/ml)

Figure 8

Figure 8. Schematic representation of the effect of MSC treatment alleviated sepsis-induced ALI by inhibiting ferroptosis and NETosis.